

ZINC VANADIUM OXIDE COUPLED CARBON NITRIDE NANOCOMPOSITE
FOR PHOTOCATALYTIC CARBON DIOXIDE REDUCTION TO METHANOL

ABDULLAH SALEM MOHAMMED BAFAQEER

A thesis submitted in fulfilment of the
requirements for the award of the degree of
Doctor of Philosophy in Chemical Engineering

School of Chemical and Energy Engineering
Faculty of Engineering
Universiti Teknologi Malaysia

SEPTEMBER 2019

To my father, mother and family members for their support and sacrifices

ACKNOWLEDGEMENT

I would like to take this opportunity to express my gratitude to Allah S.W.T for His endless mercies, blessings and guidance from birth now and forever.

Firstly, I would love to express my sincere gratitude to my supervisor Dr. Muhammad Tahir for his continuous support throughout my research, for his patience, motivation, enthusiasm, wealth of knowledge and experience. His guidance helped me a lot during my research and the writing of this dissertation. It is a great honor working as your student during my research. I would also like to appreciate my co-supervisor Prof. Dr. Nor Aishah Saidina Amin for her guidance and advices throughout my research. Aside that, I express my sincere appreciation to the Chemical Reaction Engineering Group (CREG) members and other UTM friends for their support and valuable inputs regarding this research.

Last but not least, I owe great thanks to my parents, brothers, sisters, wife and friends that supported me all the way despite the distance. No matter what decision I made, my family was always there for supporting me and pushing me forward and for that no thanks can express my gratitude.

ABSTRACT

Photocatalytic reduction of carbon dioxide (CO_2) with water (H_2O) into solar fuels is considered as a promising strategy to simultaneously address the global energy and environmental issues. The main objective of this study was to design and fabricate photoreactor system and to synthesize Z-scheme assembly of reduced graphene oxide (RGO) and protonated carbon nitride (pCN) based zinc vanadium oxide (ZnV_2O_6) nanocomposite for selective photoreduction of CO_2 to solar fuels. The pure ZnV_2O_6 , $\text{ZnV}_2\text{O}_6/\text{RGO}$, $\text{ZnV}_2\text{O}_6/\text{pCN}$ and $\text{ZnV}_2\text{O}_6/\text{RGO}/\text{pCN}$ nanocomposites were synthesized by a single step solvothermal method. The performance of nanocomposite catalysts was investigated in a liquid and gas phase photocatalytic systems under UV and visible light irradiations. The most effective catalyst in liquid phase system was $\text{ZnV}_2\text{O}_6/\text{RGO}/\text{pCN}$ which gave a maximum methanol yield of $3726.7 \mu\text{mol g-cat}^{-1}$ using photoreactor without reflector and $5207.2 \mu\text{mol g-cat}^{-1}$ using photoreactor with reflector. Performance comparison revealed 1.4 times higher yield rate in photoreactor with reflector compared to photoreactor without reflector. Besides, weight percent ratio, effect of time and stability contributed significantly to enhance reactor performances. Using gas phase system, $\text{ZnV}_2\text{O}_6/\text{RGO}/\text{pCN}$ nanocomposite demonstrated excellent photoactivity in the reduction of CO_2 into carbon monoxide (CO), hydrogen (H_2), methane (CH_4) and methanol (CH_3OH) under visible light irradiation. The CO evolution rate as a main product over $\text{ZnV}_2\text{O}_6/\text{RGO}/\text{pCN}$ nanocomposite of $3756 \mu\text{mol g-cat}^{-1}$ was obtained. The quantum efficiency of 14.2 % was achieved for CH_3OH production in a photoreactor with reflector, followed by 10.4 % and 0.25 % in photoreactor without reflector and fixed-bed photoreactor, respectively under visible light irradiation. Finally, Langmuir-Hinshelwood kinetic model was developed to investigate adsorption behaviors and photocatalytic oxidation and reduction process. In conclusion, solar photoreactor with reflector and modified ZnV_2O_6 nanocatalysts could make markedly higher CO_2 reduction to fuels.

ABSTRAK

Penurunan ber fotomangkin karbon dioksida (CO_2) bersama air (H_2O) kepada bahan api solar dianggap sebagai strategi yang baik untuk menangani isu-isu tenaga dan alam sekitar global secara serentak. Objektif utama kajian ini adalah untuk mereka bentuk dan membina sistem fotoreaktor dan untuk mensintesis pemasangan skema Z grafin oksida terturun (RGO) dan nanokomposit zink vanadium oksida (ZnV_2O_6) berasaskan karbon nitrida berproton (pCN) untuk pemilihan fotopenurunan selektif CO_2 kepada bahan api solar. Nanokomposit tulen ZnV_2O_6 , $\text{ZnV}_2\text{O}_6/\text{RGO}$, $\text{ZnV}_2\text{O}_6/\text{pCN}$ dan $\text{ZnV}_2\text{O}_6/\text{RGO}/\text{pCN}$ telah disintesis dengan kaedah solvoterma langkah tunggal. Prestasi mangkin nanokomposit telah dikaji di dalam sistem fotomangkin fasa cecair dan fasa gas di bawah penyinaran UV dan cahaya nampak. Mangkin paling berkesan di dalam sistem fasa cecair adalah $\text{ZnV}_2\text{O}_6/\text{RGO}/\text{pCN}$ yang memberikan hasil metanol maksimum sebanyak $3726.7 \mu\text{mol g-cat}^{-1}$ menggunakan fotoreaktor tanpa pemantul (reflektor) dan $5207.2 \mu\text{mol g-cat}^{-1}$ menggunakan fotoreaktor dengan pemantul. Perbandingan prestasi mendedahkan kadar hasil 1.4 kali lebih tinggi di dalam fotoreaktor dengan pemantul berbanding fotoreaktor tanpa pemantul. Selain itu, nisbah peratus berat, kesan masa dan kestabilan menyumbang kepada peningkatan prestasi reaktor yang ketara. Menggunakan sistem fasa gas, nanokomposit $\text{ZnV}_2\text{O}_6/\text{RGO}/\text{pCN}$ menunjukkan aktiviti foto yang cemerlang dalam penurunan CO_2 kepada karbon monoksida (CO), hidrogen (H_2), metana (CH_4) dan metanol CH_3OH di bawah penyinaran cahaya nampak. Kadar pembebasan CO sebagai produk utama bagi nanokomposit $\text{ZnV}_2\text{O}_6/\text{RGO}/\text{pCN}$ sebanyak $3756 \mu\text{mol g-cat}^{-1}$ telah diperoleh. Kecekapan kuantum sebanyak 14.2% telah dicapai untuk penghasilan CH_3OH di dalam fotoreaktor dengan pemantul, diikuti dengan 10.4% dan 0.25% di dalam fotoreaktor tanpa pemantul dan fotoreaktor lapisan tetap, masing-masing di bawah penyinaran cahaya nampak. Akhir sekali, model kinetik Langmuir-Hinshelwood telah dibangunkan untuk menyiasat kelakuan penyerapan dan proses pengoksidaan dan penurunan fotomangkin. Kesimpulannya, fotoreaktor solar dengan pemantul dan nanomangkin ZnV_2O_6 terubahsuai boleh melakukan penurunan CO_2 kepada bahan api yang ketara lebih tinggi.

TABLE OF CONTENTS

	TITLE	PAGE
	DECLARATION	Error! Bookmark not defined.
	DEDICATION	iii
	ACKNOWLEDGEMENT	iv
	ABSTRACT	v
	ABSTRAK	vi
	TABLE OF CONTENTS	vii
	LIST OF TABLES	xi
	LIST OF FIGURES	xii
	LIST OF ABBREVIATIONS	xvi
	LIST OF SYMBOLS	xvii
	LIST OF APPENDICES	xviii
CHAPTER 1	INTRODUCTION	1
	1.1 Problem Background	1
	1.2 Photocatalytic Reduction of Carbon Dioxide	2
	1.3 Problem Statement and Research Hypothesis	4
	1.4 Research Objectives	6
	1.5 Scope of Study	6
	1.6 Significance of Study	7
	1.7 Outline of Thesis	8
CHAPTER 2	LITERATURE REVIEW	9
	2.1 Introduction	9
	2.2 Fundamentals of Photocatalytic Process	9
	2.2.1 Principle of Photocatalysis	9
	2.2.2 Factors Affecting Photoreduction Processes	12
	2.3 Thermodynamics for Photocatalytic CO ₂ Reduction	14
	2.4 Progress towards Photoreduction of CO ₂ to Fuels	18

2.5	Graphitic Carbon nitride (g-C ₃ N ₄)	27
2.6	Zinc Vanadium Oxide (ZnV ₂ O ₄) photocatalyst	28
2.7	Reduced Graphene Oxide (RGO)	29
2.8	Z-scheme Photocatalysts	30
2.9	Characterization of Catalysts	32
2.9.1	X-ray Diffraction	33
2.9.2	Field Emission Scanning Electron Microscopy (FESEM)	34
2.9.3	X-ray Photo-electron Spectroscopy (XPS) Analysis	34
2.9.4	Transmission Electron Microscope (TEM)	35
2.9.5	Brunauer Emmett Teller (BET) Theory and Barrett Joyner Halenda (BJH)	35
2.9.6	UV-Visible Diffuse Reflectance Spectra	36
2.10	Photocatalytic Reactors for Reduction of CO ₂	36
2.10.1	Fundamentals of Photocatalytic Reactors	36
2.10.2	Progress in Photocatalytic Reactors	37
2.10.2.1	Fixed Bed Photoreactors	38
2.10.2.2	Slurry Photoreactors	40
2.11	Langmuir-Hinshelwood Kinetic Model	41
2.12	Summary	46
CHAPTER 3	RESEARCH METHODOLOGY	48
3.1	Introduction	48
3.2	Materials and Reagents	49
3.3	Catalyst Preparation	51
3.3.1	Synthesis of functionalized g-C ₃ N ₄ (pCN) nanosheets	51
3.3.2	Synthesis of ZnO/V ₂ O ₅ Composite	52
3.3.3	Synthesis of Novel 2D ZnV ₂ O ₆ Nanosheets	52
3.3.4	Synthesis of RGO-Modified ZnV ₂ O ₆ (ZnV ₂ O ₆ /RGO) Nanosheets	53
3.3.5	Synthesis of pCN-Modified ZnV ₂ O ₆ (ZnV ₂ O ₆ /pCN) Nanosheets	54

3.3.6	Synthesis of RGO and pCN Modified ZnV ₂ O ₆ (ZnV ₂ O ₆ /RGO/pCN) Nanosheets	55
3.4	Catalyst Characterization	57
3.5	Photocatalytic Activity Measurements	58
3.5.1	Solar Photoreactor and Solar Photoreactor with reflector	59
3.5.2	Fixed-bed Photoreactor	62
3.6	Gas Chromatography Analysis of Products	63
3.7	Analysis of Catalysts and Experimental Data	64
3.7.1	Calculation of Crystal Size and Band Gap Energy	64
3.7.2	Calculation of Yield Rate and Selectivity	65
3.7.3	Calculation of Quantum Efficiency	66
3.8	Kinetic Model Development	67
CHAPTER 4	RESULTS AND DISCUSSION	68
4.1	Introduction	68
4.2	Characterization of the prepared catalysts	68
4.2.1	X-ray Diffraction (XRD) Analysis	69
4.2.2	FESEM Analysis	71
4.2.3	EDX Analysis	72
4.2.4	TEM Analysis	75
4.2.5	BET Analysis	77
4.2.6	XPS Analysis	77
4.2.7	DR UV-Vis Spectrophotometry Analysis	79
4.2.8	RAMAN Analysis	82
4.2.9	PL Analysis	83
4.3	Photocatalytic CO ₂ Reduction to Methanol using Solar Photoreactor	85
4.3.1	Effect of Reaction Medium	85
4.3.2	Effect of Photo-catalysts on Yield of Methanol	86
4.3.3	Effect of Different Exposure Times of Heating for Prepared ZnV ₂ O ₆ Catalyst	88
4.3.4	Effect of pCN Loading on ZnV ₂ O ₆ Photoactivity	89

4.3.5	Effect of RGO Loading on ZnV ₂ O ₆ /pCN Photoactivity	90
4.3.6	Effect of Irradiation Time on Methanol Yield	91
4.3.7	Stability Study of Various Photocatalysts for CO ₂ Conversion to Methanol	92
4.4	Photocatalytic CO ₂ Reduction to Methanol using Solar Photoreactor with Reflector	93
4.4.1	Effect of Catalyst Loading on Methanol Yield	94
4.4.2	Effect of Irradiation Time on Methanol Yield	95
4.4.3	Performance Comparison of Solar Photoreactor and Solar Photoreactor with Reflector	97
4.5	Photocatalytic CO ₂ Reduction to Solar Fuels using Fixed-bed Photoreactor	98
4.5.1	Performance Comparison of Solar-light and UV-light over Various Photocatalysts	99
4.5.2	Performance Analysis of Photo-catalysts	101
4.5.3	Effect of Irradiation Time on Products Yield	102
4.6	Quantum Efficiency Analysis	106
4.7	Mechanism of Reaction	108
4.8	Development of Kinetic Model	111
4.9	Summary	117
CHAPTER 5	CONCLUSION AND RECOMMENDATIONS	120
5.1	Conclusions	120
5.2	Recommendations for Future Research	122
	REFERENCES	124
	APPENDICES	140

LIST OF TABLES

TABLE NO.	TITLE	PAGE
Table 2.1	Previous researches on photoreduction of CO ₂ with H ₂ O to solar fuels from 2010 till date (Liquid phase)	20
Table 3.1	Type of materials used for catalyst synthesis	50
Table 3.2	Types of gases used during experimental work	50
Table 4.1	Physical properties of the samples	77
Table 4.2	Summary of band gap energy of samples	82
Table 4.3	Summary of yield rates and selectivity over various catalysts	102
Table 4.4	Summary of yield rates and quantum yield over ZnV ₂ O ₆ /RGO/pCN	107
Table 4.5	Summary of kinetic constants for fitting model with experimental data	117

LIST OF FIGURES

FIGURE NO.	TITLE	PAGE
Figure 2.1	Schematic representation of the “band gap model.” (1) Photoinduced electron-hole pair creation; (2) charge migration to the surface; (3) Photocatalytic oxidation and reduction processes; (4) recombination. VB and CB represent valence band and conduction band, respectively.	10
Figure 2.2	Thermodynamics and Gibbs free energy (G) of semiconductor under light and without light.	16
Figure 2.3	Expansion and narrowing of band gap of semiconductors [64].	17
Figure 2.4	Band positions of various semiconductor photocatalysts and the redox potentials of CO ₂ reduction at pH 7) [65].	18
Figure 2.5	Direct Z-scheme g-C ₃ N ₄ /ZnO binary composite photocatalytic system was constructed and exhibited enhanced photocatalytic CO ₂ reduction activity than g-C ₃ N ₄ or ZnO [125].	31
Figure 2.6	Indirect Z-scheme g-C ₃ N ₄ /RGO/BiVO ₄ composite [24].	32
Figure 2.7	Classification of photoreactors design used for the photocatalytic CO ₂ reduction to solar fuels.	38
Figure 2.8	(a) Schematic of Cylindrical Quartz tube photoreactor[132]; (b) Schematic of Vertical Tubular Fixed Bed Photoreactor [133]; (c) Schematic of Internal-Illuminated Monolith Photoreactor [134].	40
Figure 2.9	(a) Schematic of photocatalytic reduction system irradiated from top [135]; (b) Schematic of Internally Illuminated Annular Photoreactor [136].	41
Figure 3.1	Flow chart of general research methodology	49
Figure 3.2	Solvothermal preparations of ZnV ₂ O ₆ nanosheets	53
Figure 3.3	Solvothermal method for preparation of RGO-modified ZnV ₂ O ₆ nanosheets	54
Figure 3.4	Solvothermal method for preparation of pCN-modified ZnV ₂ O ₆ nanosheets	55
Figure 3.5	Solvothermal method for preparation of RGO and pCN modified ZnV ₂ O ₆ nanosheets	56

Figure 3.6	Schematic of experimental set-up for CO ₂ reduction in a solar photoreactor under visible light (Liquid phase)	61
Figure 3.7	Experimental rig of solar photoreactor system for photocatalytic CO ₂ reduction (Liquid phase)	61
Figure 3.8	Schematic of experimental set-up using solar photoreactor with reflector for photocatalytic CO ₂ reduction (Liquid phase)	62
Figure 3.9	Schematic of experimental set-up using solar photoreactor with reflector for photocatalytic CO ₂ reduction (Liquid phase)	62
Figure 3.10	Schematic of experimental set-up for photo-catalytic CO ₂ in presence of H ₂ O in a fixed-bed photoreactor	63
Figure 4.1	XRD pattern of ZnV ₂ O ₆ nanosheets and ZnV ₂ O ₆ calcined	69
Figure 4.2	XRD pattern of RGO, pCN, ZnV ₂ O ₆ , ZnV ₂ O ₆ /RGO (4%), ZnV ₂ O ₆ /pCN (50%), ZnV ₂ O ₆ /pCN (100%) and ZnV ₂ O ₆ /RGO(4%)/pCN(100%) samples	70
Figure 4.3	FE-SEM images of (a) pCN; (b) ZnV ₂ O ₆ after 12 h; (c) ZnV ₂ O ₆ after 24 h; (d) Calcined ZnV ₂ O ₆ after 24 h; (e) ZnV ₂ O ₆ /RGO (4%); (f) ZnV ₂ O ₆ /pCN (100%); (g and h) ZnV ₂ O ₆ /RGO(4%)/pCN(100%)	72
Figure 4.4	EDX mapping analysis of RGO modified ZnV ₂ O ₆ nanosheets: (a, b) EDX mapping of ZnV ₂ O ₆ /RGO, (c) EDX analysis of ZnV ₂ O ₆ /RGO sample	73
Figure 4.5	EDX mapping analysis of pCN modified ZnV ₂ O ₆ nanosheets: (a) ZnV ₂ O ₆ /pCN nanosheets, (b) EDX mapping of ZnV ₂ O ₆ /pCN, (c) EDX plots with elements composition	74
Figure 4.6	SEM micrographs of RGO modified ZnV ₂ O ₆ /pCN nanosheets: (a) ZnV ₂ O ₆ /RGO/pCN samples; (b and c) EDX mapping of ZnV ₂ O ₆ /RGO/pCN	75
Figure 4.7	TEM images of (a) pCN; (b) 2D ZnV ₂ O ₆ ; (c) RGO; (d) ZnV ₂ O ₆ /RGO (4%) nanosheets; (e) ZnV ₂ O ₆ /pCN (100%) nanosheets; (f) ZnV ₂ O ₆ /RGO(4%)/pCN sample; (g) d-spacing of ZnV ₂ O ₆ /RGO(4%)/pCN sample; (h) SAED pattern of the ZnV ₂ O ₆ /RGO(4%)/pCN sample	76
Figure 4.8	XPS spectra of ZnV ₂ O ₆ /RGO(4%)/pCN(100%): (a) survey spectrum; (b) V 2p; (c) Zn 2p; (d) O 1s; (e) C 1s and (f) N 1s	78
Figure 4.9	UV–vis diffuse reflectance absorbance spectra of pCN, 2D ZnV ₂ O ₆ , calcined ZnV ₂ O ₆ , ZnO/V ₂ O ₅ , ZnV ₂ O ₆ /pCN	

	(50%), ZnV ₂ O ₆ /pCN (100%), ZnV ₂ O ₆ /RGO (4%) and ZnV ₂ O ₆ /RGO(4%)/pCN(100%) samples	80
Figure 4.10	Valence band (VB) XPS spectra of ZnV ₂ O ₆	81
Figure 4.11	Valence band (VB) XPS spectra of pCN	81
Figure 4.12	Raman spectra of pCN, ZnV ₂ O ₆ , RGO, ZnV ₂ O ₆ /pCN (50%), ZnV ₂ O ₆ /pCN (100%), ZnV ₂ O ₆ /RGO (4%) and ZnV ₂ O ₆ /RGO(4%)/pCN(100%) samples; (b) Photoluminescence (PL) spectra for pCN, ZnV ₂ O ₆ , calcined ZnV ₂ O ₆ , RGO, ZnV ₂ O ₆ /pCN (50%), ZnV ₂ O ₆ /pCN	83
Figure 4.13	Photoluminescence (PL) spectra for pCN, ZnV ₂ O ₆ , calcined ZnV ₂ O ₆ , RGO, ZnV ₂ O ₆ /pCN (50%), ZnV ₂ O ₆ /pCN (100%), ZnV ₂ O ₆ /RGO (4%) and ZnV ₂ O ₆ /RGO(4%)/pCN(100%) samples	84
Figure 4.14	Methanol yield for different reaction mediums (Irradiation time 2h)	86
Figure 4.15	Methanol yield over various photo-catalysts (Irradiation time 2 h)	87
Figure 4.16	Effect of different exposure times of heating for 12 h, 24 h, 48 h and 72 h for prepared ZnV ₂ O ₆ catalyst for CO ₂ photo reduction (Irradiation time 2 h)	88
Figure 4.17	Effects of pCN loading on ZnV ₂ O ₆ photoactivity for photocatalytic CO ₂ reduction to methanol (Irradiation time 2 h)	89
Figure 4.18	Effects of RGO loading on ZnV ₂ O ₆ /pCN photoactivity for photocatalytic CO ₂ reduction to methanol (Irradiation time 2 h)	91
Figure 4.19	Effect of irradiation time on photocatalytic CO ₂ reduction to methanol over various photo-catalysts	92
Figure 4.20	Stability study of ZnV ₂ O ₆ , ZnV ₂ O ₆ /pCN (100%), ZnV ₂ O ₆ /RGO (4%) and ZnV ₂ O ₆ /RGO(4%)/pCN(100%) samples for CO ₂ conversion to methanol	93
Figure 4.21	The effect of catalyst loading over ZnV ₂ O ₆ /RGO(4%)/pCN(100%) composite (Room temperature, feed flow rate 20 mL/min and irradiation time 2 h)	95
Figure 4.22	Effect of irradiation time for photocatalytic CO ₂ reduction with H ₂ O to methanol over various catalysts	96
Figure 4.23	Schematic illustration of heterojunction structures for (a) 2D ZnV ₂ O ₆ nanosheets; (b) ZnV ₂ O ₆ /g-C ₃ N ₄	

	heterojunction; (c) $\text{ZnV}_2\text{O}_6/\text{g-C}_3\text{N}_4$ heterojunction with functionalization (HNO_3) as a mediator; and (d) $\text{ZnV}_2\text{O}_6/\text{RGO}/\text{g-C}_3\text{N}_4$ heterojunction with RGO and functionalization (HNO_3) as multiple mediators	97
Figure 4.24	Performance comparisons between Solar Photoreactor without Reflector and Solar Photoreactor with Reflector over ZnV_2O_6 and $\text{ZnV}_2\text{O}_6/\text{RGO}/\text{pCN}$ catalysts	98
Figure 4.25	Production rate of CO , CH_3OH , H_2 and CH_4 during CO_2 reduction for various catalysts under (a) solar-light; (b) UV-light irradiations (Irradiation time 1 h)	100
Figure 4.26	Performance analysis of photo-catalysts for selective production of CO under solar-light irradiation (Irradiation time 1 h)	101
Figure 4.27	CO yield for UV and solar light against irradiation time over $\text{ZnV}_2\text{O}_6/\text{RGO}(4\%)/\text{pCN}(100\%)$ composite	103
Figure 4.28	CH_4 yield for UV and solar light against irradiation time over $\text{ZnV}_2\text{O}_6/\text{RGO}/\text{pCN}$ composite	104
Figure 4.29	H_2 yield for UV and solar light against irradiation time over $\text{ZnV}_2\text{O}_6/\text{RGO}/\text{pCN}$ composite	105
Figure 4.30	Methanol yield for UV and solar light against irradiation time over $\text{ZnV}_2\text{O}_6/\text{RGO}/\text{pCN}$ composite	106
Figure 4.31	Diagram of (a) type-II band alignment mechanism of $\text{ZnV}_2\text{O}_6/\text{pCN}$ composite, and (b) Z-Scheme electron transfer mechanism of $\text{ZnV}_2\text{O}_6/\text{RGO}/\text{pCN}$ composite under solar light irradiation	110
Figure 4.32	Comparison of the proposed kinetic model fitting-well with the empirical profile of CO formation from photocatalytic CO_2 reduction with H_2O	116

LIST OF ABBREVIATIONS

DMF	-	N,N-dimethyl formamide
RGO	-	Reduced graphene oxide
pCN	-	Protonated carbon nitride
ZnV ₂ O ₄	-	Zinc vanadium oxide
g-C ₃ N ₄	-	Graphitic carbon nitride
CO ₂	-	Carbon dioxide
GHG	-	Greenhouse gas
VB	-	Valence Band
CB	-	Conduction Band
FESEM	-	Field Emission Scanning Electron Microscopy
BET	-	Braunauer-Emmer-Teller
XRD	-	X-ray Diffraction
PL	-	Photoluminescence
UV/Vis	-	Ultraviolet Visible
XPS	-	X-ray Photoelectron spectroscopy
HRTEM	-	High Resolution Transmission Electron Microscopy
EDX	-	Energy Dispersive Electron Microscope
FID	-	Flame Ionization Detector
GC	-	Gas Chromatography
2D	-	Two-Dimensional
C	-	Concentration

LIST OF SYMBOLS

λ	-	Wavelength
f	-	Photon flux
e^-	-	Electron
h^+	-	Hole
P	-	Pressure
α	-	Alpha
β	-	Beta
θ	-	Theta
Φ	-	phi
E_{bg}	-	Energy band gap
E	-	Activation energy
E_p	-	Energy of photon
h	-	Planks constant
ΔH	-	Change in enthalpy of reaction (KJ/mole)
H	-	Heat of reaction
I	-	Light intensity (mW/cm^2)
I_p	-	Photon Irradiance
k	-	Reaction rate constant
k_1	-	Reduction rate constant
k_2	-	Oxidation rate constant
KJ	-	Kilo Joule
L	-	Length
μm	-	Micrometer
W	-	Watt
T	-	Temperature

LIST OF APPENDICES

APPENDIX	TITLE	PAGE
Appendix A	List of scientific publications, patents and awards	140
Appendix B	Photographs of photocatalytic reactors	142
Appendix C	Photographs of modified nanocatalysts and liquid phase products	145
Appendix D	Hromatographs peaks	147
Appendix E	Procedure for calculations	149
Appendix F	Explanation of polymath and simulation	153

CHAPTER 1

INTRODUCTION

1.1 Problem Background

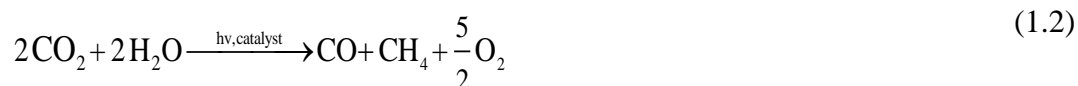
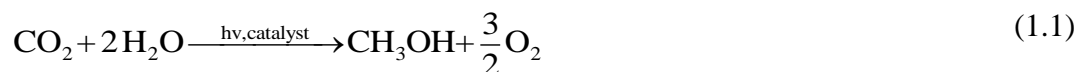
Climate change because of global warming arising from the emission of greenhouse gas carbon dioxide (CO₂) poses a severe threat to our future [1, 2]. Combustion of fossil fuel is the main source of greenhouse gas emission especially CO₂, which ultimately leads to global warming [3]. Furthermore, greenhouse gases contribute many negative influences such as loss in biodiversity, occurrence of acid rain and increase in sea level [4]. Exploring new energy resources are inevitable to address shortage in fossil fuels supply, continuous increase in energy demand and pressing environmental issues [5]. Recently, many efforts were endorsed to decrease CO₂ emission through pre or post combustions and also capturing and sequestration. However, these processes are energy intensive, thus uneconomical [6].

Using easily available and renewable carbon resource like CO₂ for improvement of carbon-based fuels is imperative for the sustainability, since CO₂ is totally abundant, cheap and green as well as a renewable feedstock [7]. During the last decade, different types of technologies were investigated for CO₂ reforming to carbon-based fuels namely, plasma reforming, thermal reforming and photoreduction [8]. However, the biggest obstacle for establishing industrial processes based on CO₂ is its low energy level. CO₂ is a stable molecule that requires high energy to convert it into fuels. Therefore, technologies pertinent to carbon management, which not only alleviate global temperature, but also meet increasing energy demands economically, are high in the priority list [9]. Recently, photocatalytic CO₂ reduction has gained significant importance toward production of solar fuels like CH₃OH, CO and CH₄ [10-12]. The phototechnology has high potential for reducing CO₂ emission and partly overcoming energy crises [13, 14]. Therefore, the photoreduction of CO₂ utilizing

visible light illuminations could be a potential pathway for the sustainability of the society.

1.2 Photocatalytic Reduction of Carbon Dioxide

Photocatalytic reduction of CO₂ is one of the most promising solutions to both global warming and energy crises, since CO₂ can be reduced to solar fuels at relatively low temperature and atmospheric pressure [15, 16]. In recent innovations, the ubiquitous photocatalysis has gained increasing attention as it can operate at normal operating conditions. During photocatalytic reduction of CO₂ to solar fuels, energy requirement could be provided using sunlight which is a green source of energy. In this technology, stability of catalyst and its performance is affirmed because of mild operating conditions. The photoreduction of CO₂ by using water (H₂O) as reductant are stated in Equations (1.1) - (1.2).



When CO₂ reacts with H₂O in a three phase heterogeneous slurry system (gas, liquid and solid), CH₃OH prevailed during photocatalytic CO₂ reduction with H₂O in a slurry system as explained in Equation (1.1). Using two phase heterogeneous system (gas and solid), CO and CH₄ are produced as explained in Equation (1.2). Equation (1.1) - (1.2) revealed renewable fuels such as CH₃OH, CO and CH₄ can be produced in a single step. Hence, these reactions affirmed phototechnology as the most attractive and a future hope for mitigation of greenhouse gas with production of green fuels for sustainable development [14].

Among various semiconductors, the focus has been on graphitic carbon nitride (g-C₃N₄) as a photocatalyst. g-C₃N₄ has been researched excessively over the past decades due to its encouraging advantages including elemental abundance, high chemical and thermal stability, appropriate band gap energy and eco-friendly nature [17]. However, the performance of g-C₃N₄ is still restricted because of its high recombination rate of photo-produced electron and hole pairs [18-21]. The efficiency of g-C₃N₄ can be improved by exfoliation and functionalization. Several efforts were made to promote the efficiency of g-C₃N₄ like doping with metal and non-metal elements [22], engineering approach [23] and coupling with other semiconductors [24-27]. RGO with two-dimensional structure is one of the most promising mediator/modifier due to its excellent electron mobility and higher light absorption [28, 29]. Modification of g-C₃N₄ with RGO has exhibited considerable progress due to it promotes separation of charges. Thus, numerous research efforts were made to improve g-C₃N₄ efficiency such as RGO/protonated g-C₃N₄ [30], RGO/g-C₃N₄ [31], RGO/g-C₃N₄ [32] and g-C₃N₄/GO [33]. Therefore, it is appropriate to develop g-C₃N₄/RGO based semiconductors for enhanced photocatalytic CO₂ reduction applications under solar energy.

In the current development, ternary nanostructures like nanoplates, nanosheets, microspheres and nanorods have gained much attention and exhibited magnificent performances in photo-induced CO₂ reduction and other energy applications [34-36]. Moreover, the construction of Z-scheme photo-induced system has received much attention because of its ideal effectiveness in improving the photo-induced efficiency [37]. Therefore, developing ternary zinc-vanadium oxide nanostructures could enhance both photoactivity and selectivity. Recently, zinc-vanadium oxide (ZnV₂O₄) has gained attention because of its interesting structural changes at low temperatures [38]. Different nanostructures of ZnV₂O₄ have been reported like hollow spheres, clewlike hollow structures, nanosheets, and glomerulus nano/microspheres for various applications [39-41]. However, structured ZnV_xO_y based photo-catalyst has never been reported for photo-induced CO₂ reduction application.

Therefore, it is appropriate to explore ternary ZnV₂O₆ semiconductor for photocatalytic CO₂ reduction applications under solar energy. Combining 2D ZnV₂O₆

nanosheets with rGO/g-C₃N₄ composite would develop indirect Z-scheme heterojunction which may not only increase charges separation performance but also provides good redox potential for selective CO₂ reduction under visible light. Thus, it is extremely desirable to construct g-C₃N₄ modified RGO/ZnV₂O₆ composite to improve photo-induced conversion of CO₂ into fuels under visible light illuminations.

During the last decade, optical fiber reactors have been under investigation for photoreduction of CO₂. The optical fiber reactors fall in the category of efficient photocatalytic reactors. These reactors have been explored for photocatalytic reduction of CO₂, since the exposed surface area to light ratio are larger, delivering light efficiently and uniformly throughout the reactor [42, 43]. However, several disadvantages such as lower adhesion strength and relatively low surface area limited their applications [44, 45].

Among the photocatalytic reactors, the solar photoreactor with large illuminated surface area and efficient light utilization/distribution over the catalyst surface are considerably effective for photocatalytic CO₂ reduction applications. Basically, the solar photo-reactors are the most frequently utilized and involve three phase system where the catalyst bed is in a fluidized form and agitated to increase mass transfer between catalyst and reactants, thus providing high surface area to be illuminated [46]. In addition, higher light distribution and harvesting over the catalyst surface would also be possible utilizing reflector. Therefore, solar photoreactor with reflector could make higher CO₂ reduction to solar fuels with higher selectivity.

1.3 Problem Statement and Research Hypothesis

Conversion of CO₂ to solar fuels provides alternative ways for monitoring global warming and energy crises. The main challenges ahead in this field are described as below:

- (a) Thermal conversion of CO₂ to solar fuels is a two-step process which required higher input energy. Therefore, the single step CO₂ reduction to hydrocarbon

fuels is possible through photo-technology process. Photoreduction of CO₂ with H₂O would be possible at normal temperature and pressure using solar energy.

- (b) Although, photoreduction of CO₂ to fuels through photocatalytic reductions have several advantages, yet photocatalysts under investigations are inefficient to produce solar fuels with sufficient yield rates and selectivity. Among semiconductor materials, g-C₃N₄ is widely investigated because of abundantly availability, comparatively cheap and numerous other advantageous. However, it has lower light absorption efficiency, trivial photoactivity and selectivity for photocatalytic CO₂ reduction to solar fuels. Thus, photocatalytic efficiency of g-C₃N₄ can further be improved by combining with other semiconductor materials.
- (c) Novel semiconductor ZnV₂O₆ would be the best candidate to be combined with g-C₃N₄ because of sufficient E_{CB} and E_{VB} potential for the conversion of CO₂ to fuels. ZnV₂O₆ has been investigated intensively owing to their unique physical and chemical properties including efficiently utilize the visible region of the solar spectrum owing to narrow band gap. However, it has never been reported for photoreduction of CO₂ to solar fuels under visible light irradiation. Besides, introduction of RGO onto the both semiconductors will provide Z-scheme photocatalytic system that can promote the photocatalytic conversion of CO₂ to fuel production to the ultimate point.
- (d) Existing photoreactors have lower quantum efficiency because of inefficient harvesting and distribution of light irradiation over the catalyst surface. In addition, such types of reactors have lower exposed surface area, lower catalyst loading, and ineffective adsorption-desorption process and less mass transfer over the catalyst surface, resulting in lower yield rate and selectivity. Therefore, solar photoreactor will be productive to provide higher illuminated active surface area, higher adsorption-desorption and efficient mass transfer toward catalyst surface. Higher light distribution and harvesting over the catalyst surface would also be possible utilizing reflector, ultimately stimulating higher quantum efficiency toward efficient CO₂ reduction to selective solar fuels.

1.4 Research Objectives

The aim of this research is to design a solar photoreactor with reflector having cooling system and capable of enhancing CO₂ reduction and yield rates. Next novel nanocatalysts and process operating parameters are deliberated to maximize CO₂ reduction efficiency. The specific objectives of the research are:

- (a) To synthesize and characterize Z-scheme rGO and g-C₃N₄ based ZnV₂O₆ nanocatalysts for solar energy applications;
- (b) To test the performance of nanocatalysts for selective CO₂ photoreduction to solar fuels;
- (c) To investigate and compare the performance of photoreactors for selective photocatalytic CO₂ conversion to solar fuels under UV and visible light irradiations;
- (d) To determine kinetic and reaction rate parameters for understanding the role of nanocatalysts toward optimization of CO₂ reduction process.

1.5 Scope of Study

The scopes of this study are focused on resolving some of the fundamental problems related to lower CO₂ reduction efficiency and selectivity. In this perspective, synthesis and characterization of various nanocatalysts, reaction mechanisms of CO₂ reduction, oxidative-reductive model development and quantum efficiency analysis have been deliberated. Furthermore, the design of photoreactor is limited to the fabricating of solar photoreactor with reflector to maximize yield rates and products selectivity. The CO₂ reduction efficiency is related to maximize yield rates of desired products. Therefore, the specific research scope of this study is as follows:

- (a) Novel ZnV₂O₆ nanosheets, ZnV₂O₆/g-C₃N₄ nanosheets, RGO combined ZnV₂O₆ nanosheets and Z-scheme ZnV₂O₆/RGO/g-C₃N₄ nanosheets photocatalysts are synthesized using one-step solvothermal method to

investigate the route of CO₂ photo-reduction to solar fuels. Nanocatalysts characterization are conducted using XRD, BET, FESEM, EDX, HRTEM, XPS, UV-Visible, RAMAN and PL spectroscopy in order to investigate the phase and crystal structure, surface morphology and mesoporosity, surface area and pore size distribution, metals transitions states and optical properties of catalysts.

- (b) The role of nanocatalysts for photocatalytic reduction of CO₂ to solar fuels was firstly explored using solar photoreactor in which catalyst was distributed in the slurry aqueous system. The light source used was a 35W HID Xe lamp with a light intensity of 20 mWcm⁻² operated using high voltage power supply. The reducing agent employed was H₂O for CO₂ photo-reduction.
- (c) In solar photoreactor design, a reflector was used to reflect the light to provide higher light irradiations to get higher reduction and yield rates. The photocatalytic reduction of CO₂ to solar fuels was investigated using H₂O as reducing agents. The performance comparison between fixed-bed (gas phase), solar photoreactor (liquid phase) and solar photoreactor with reflector (liquid phase) was conducted to investigate the efficiency of solar photoreactor with reflector.
- (d) The catalysts were then used to photo-reduce CO₂ to obtain solar fuels using both UV and Visible light and their performances were compared based on the yield of fuels. The reaction mechanism and kinetic model were developed to find out the key parameters in CO₂ reduction applications.

1.6 Significance of Study

In this study, CO₂ was efficiency converted to CH₃OH, CO, CH₄ and H₂ in the presence of reducing agents and photocatalytic systems, thus confirming sustainable fuel productions. The solar photoreactor with reflector performance was very encouraging while the efficiency found was much higher than ever reported in the literature. However, several outcomes of this research are described below:

- (a) New solar photoreactor with reflector system to investigate efficient CO₂ reduction to solar fuels.
- (b) Novel ZnV₂O₆ nanosheets for stable and high-performance photo-induced CO₂ reduction to solar fuels.
- (c) Novel indirect Z-scheme assembly of ZnV₂O₆/RGO/g-C₃N₄ nanosheets toward visible-light enhanced CO₂ reduction.
- (d) New development in reaction rate and kinetic models.
- (e) Alternative solutions to global warming and energy crises.

1.7 Outline of Thesis

This thesis is divided into five chapters excluding all introductory pages, table of content and abstract. Chapter 1 presents the introduction, problem statement and research hypothesis, objectives, research scope, significance of study and outline of thesis. The literature survey, basics of photocatalysis and CO₂ photoreduction, previous works in photoreduction of CO₂, the photoreactor setups, characterization techniques, description of photocatalytic reactors and development of kinetic models were discussed in Chapter 2. Chapter 3 gives a detailed representation of the research methodology and order of the research, details of the methods used to synthesize the catalysts and carry out the photoreduction process. The results obtained from the experiments and analysis of characterization are discussed in Chapter 4. Chapter 5 concludes the thesis with inferences drawn and recommendations for further research.

REFERENCES

1. Wang, Y., Y. Zeng, S. Wan, S. Zhang, and Q. Zhong, Construction of octahedral BiFeWO_x encapsulated in hierarchical In₂S₃ core@ shell heterostructure for visible-light-driven CO₂ reduction. *Journal of CO₂ Utilization*, 2019. 29: p. 156-162.
2. Zhao, Y., Y. Wei, X. Wu, H. Zheng, Z. Zhao, J. Liu, and J. Li, Graphene-wrapped Pt/TiO₂ photocatalysts with enhanced photogenerated charges separation and reactant adsorption for high selective photoreduction of CO₂ to CH₄. *Applied Catalysis B: Environmental*, 2018. 226: p. 360-372.
3. Nowotny, J., J. Dodson, S. Fiechter, T.M. Gür, B. Kennedy, W. Macyk, T. Bak, W. Sigmund, M. Yamawaki, and K.A. Rahman, Towards global sustainability: Education on environmentally clean energy technologies. *Renewable and Sustainable Energy Reviews*, 2018. 81: p. 2541-2551.
4. Bai, Y., P. Yang, L. Wang, B. Yang, H. Xie, Y. Zhou, and L. Ye, Ultrathin Bi₄O₅Br₂ nanosheets for selective photocatalytic CO₂ conversion into CO. *Chemical Engineering Journal*, 2019. 360: p. 473-482.
5. Liang, M., T. Borjigin, Y. Zhang, B. Liu, H. Liu, and H. Guo, Controlled assemble of hollow heterostructured g-C₃N₄@CeO₂ with rich oxygen vacancies for enhanced photocatalytic CO₂ reduction. *Applied Catalysis B: Environmental*, 2019. 243: p. 566-575.
6. Zhang, Q., Y. Li, E.A. Ackerman, M. Gajdardziska-Josifovska, and H. Li, Visible light responsive iodine-doped TiO₂ for photocatalytic reduction of CO₂ to fuels. *Applied Catalysis A: General*, 2011. 400(1-2): p. 195-202.
7. Wang, H., L. Zhang, K. Wang, X. Sun, and W. Wang, Enhanced photocatalytic CO₂ reduction to methane over WO₃· 0.33 H₂O via Mo doping. *Applied Catalysis B: Environmental*, 2019. 243: p. 771-779.
8. VijayaVenkataRaman, S., S. Iniyan, and R. Goic, A review of climate change, mitigation and adaptation. *Renewable and Sustainable Energy Reviews*, 2012. 16(1): p. 878-897.
9. Li, X., H. Liu, D. Luo, J. Li, Y. Huang, H. Li, Y. Fang, Y. Xu, and L. Zhu, Adsorption of CO₂ on heterostructure CdS (Bi₂S₃)/TiO₂ nanotube

- photocatalysts and their photocatalytic activities in the reduction of CO₂ to methanol under visible light irradiation. *Chemical Engineering Journal*, 2012. 180: p. 151-158.
10. Xu, D., B. Cheng, W. Wang, C. Jiang, and J. Yu, Ag₂CrO₄/g-C₃N₄/graphene oxide ternary nanocomposite Z-scheme photocatalyst with enhanced CO₂ reduction activity. *Applied Catalysis B: Environmental*, 2018. 231: p. 368-380.
 11. Sekizawa, K., S. Sato, T. Arai, and T. Morikawa, Solar-Driven Photocatalytic CO₂ Reduction in Water Utilizing a Ruthenium Complex Catalyst on p-Type Fe₂O₃ with a Multiheterojunction. *ACS Catalysis*, 2018. 8(2): p. 1405-1416.
 12. Wang, S., B.Y. Guan, and X.W.D. Lou, Rationally designed hierarchical N-doped carbon@ NiCo₂O₄ double-shelled nanoboxes for enhanced visible light CO₂ reduction. *Energy & Environmental Science*, 2018. 11(2): p. 306-310.
 13. Di, J., X. Zhao, C. Lian, M. Ji, J. Xia, J. Xiong, W. Zhou, X. Cao, Y. She, and H. Liu, Atomically-thin Bi₂MoO₆ nanosheets with vacancy pairs for improved photocatalytic CO₂ reduction. *Nano Energy*, 2019.
 14. Yang, C., Q. Li, Y. Xia, K. Lv, and M. Li, Enhanced visible-light photocatalytic CO₂ reduction performance of ZnIn₂S₄ microspheres by using CeO₂ as cocatalyst. *Applied Surface Science*, 2019. 464: p. 388-395.
 15. Christoforidis, K.C. and P. Fornasiero, Photocatalysis for Hydrogen Production and CO₂ Reduction: The Case of Copper-Catalysts. *ChemCatChem*, 2019. 11(1): p. 368-382.
 16. Ding, J., X. Liu, M. Shi, T. Li, M. Xia, X. Du, R. Shang, H. Gu, and Q. Zhong, Single-atom silver–manganese catalysts for photocatalytic CO₂ reduction with H₂O to CH₄. *Solar Energy Materials and Solar Cells*, 2019. 195: p. 34-42.
 17. He, Y., Y. Wang, L. Zhang, B. Teng, and M. Fan, High-efficiency conversion of CO₂ to fuel over ZnO/g-C₃N₄ photocatalyst. *Applied Catalysis B: Environmental*, 2015. 168: p. 1-8.
 18. Liu, C., H. Huang, L. Ye, S. Yu, N. Tian, X. Du, T. Zhang, and Y. Zhang, Intermediate-mediated strategy to horn-like hollow mesoporous ultrathin g-C₃N₄ tube with spatial anisotropic charge separation for superior photocatalytic H₂ evolution. *Nano Energy*, 2017. 41: p. 738-748.
 19. Li, F.-t., Y.-b. Xue, B. Li, Y.-j. Hao, X.-j. Wang, R.-h. Liu, and J. Zhao, Precipitation synthesis of mesoporous photoactive Al₂O₃ for constructing g-

- C₃N₄-based heterojunctions with enhanced photocatalytic activity. *Industrial & Engineering Chemistry Research*, 2014. 53(50): p. 19540-19549.
20. Li, W., C. Feng, S. Dai, J. Yue, F. Hua, and H. Hou, Fabrication of sulfur-doped g-C₃N₄/Au/CdS Z-scheme photocatalyst to improve the photocatalytic performance under visible light. *Applied Catalysis B: Environmental*, 2015. 168: p. 465-471.
 21. Di, T., B. Zhu, B. Cheng, J. Yu, and J. Xu, A direct Z-scheme g-C₃N₄/SnS₂ photocatalyst with superior visible-light CO₂ reduction performance. *Journal of Catalysis*, 2017. 352: p. 532-541.
 22. Adekoya, D.O., M. Tahir, and N.A.S. Amin, g-C₃N₄/(Cu/TiO₂) nanocomposite for enhanced photoreduction of CO₂ to CH₃ OH and HCOOH under UV/visible light. *Journal of CO₂ Utilization*, 2017. 18: p. 261-274.
 23. Niu, P., L. Zhang, G. Liu, and H.M. Cheng, Graphene-like carbon nitride nanosheets for improved photocatalytic activities. *Advanced Functional Materials*, 2012. 22(22): p. 4763-4770.
 24. Jiang, D., P. Xiao, L. Shao, D. Li, and M. Chen, RGO-Promoted All-Solid-State g-C₃N₄/BiVO₄ Z-Scheme Heterostructure with Enhanced Photocatalytic Activity toward the Degradation of Antibiotics. *Industrial & Engineering Chemistry Research*, 2017. 56(31): p. 8823-8832.
 25. Xia, P., B. Zhu, B. Cheng, J. Yu, and J. Xu, 2D/2D g-C₃N₄/MnO₂ nanocomposite as a direct Z-scheme photocatalyst for enhanced photocatalytic activity. *ACS Sustainable Chem. Eng.*, 2017. 6(1): p. 965-973.
 26. Miao, X., X. Shen, J. Wu, Z. Ji, J. Wang, L. Kong, M. Liu, and C. Song, Fabrication of an all solid Z-scheme photocatalyst g-C₃N₄/GO/AgBr with enhanced visible light photocatalytic activity. *Applied Catalysis A: General*, 2017. 539: p. 104-113.
 27. Katsumata, H., T. Sakai, T. Suzuki, and S. Kaneco, Highly efficient photocatalytic activity of g-C₃N₄/Ag₃PO₄ hybrid photocatalysts through Z-scheme photocatalytic mechanism under visible light. *Industrial & Engineering Chemistry Research*, 2014. 53(19): p. 8018-8025.
 28. Wang, X., L. Yin, and G. Liu, Light irradiation-assisted synthesis of ZnO–CdS/reduced graphene oxide heterostructured sheets for efficient photocatalytic H₂ evolution. *Chemical Communications*, 2014. 50(26): p. 3460-3463.

29. Fan, W., X. Yu, H.-C. Lu, H. Bai, C. Zhang, and W. Shi, Fabrication of TiO₂/RGO/Cu₂O heterostructure for photoelectrochemical hydrogen production. *Applied Catalysis B: Environmental*, 2016. 181: p. 7-15.
30. Ong, W.-J., L.-L. Tan, S.-P. Chai, S.-T. Yong, and A.R. Mohamed, Surface charge modification via protonation of graphitic carbon nitride (g-C₃N₄) for electrostatic self-assembly construction of 2D/2D reduced graphene oxide (rGO)/g-C₃N₄ nanostructures toward enhanced photocatalytic reduction of carbon dioxide to methane. *Nano Energy*, 2015. 13: p. 757-770.
31. Yu, K., X. Hu, K. Yao, P. Luo, X. Wang, and H. Wang, Preparation of an ultrathin 2D/2D rGO/g-C₃N₄ nanocomposite with enhanced visible-light-driven photocatalytic performance. *RSC Advances*, 2017. 7(58): p. 36793-36799.
32. Gu, Y., Y. Yu, J. Zou, T. Shen, Q. Xu, X. Yue, J. Meng, and J. Wang, The ultra-rapid synthesis of rGO/g-C₃N₄ composite via microwave heating with enhanced photocatalytic performance. *Materials Letters*, 2018. 232: p. 107-109.
33. Tang, L., C.-t. Jia, Y.-c. Xue, L. Li, A.-q. Wang, G. Xu, N. Liu, and M.-h. Wu, Fabrication of compressible and recyclable macroscopic g-C₃N₄/GO aerogel hybrids for visible-light harvesting: a promising strategy for water remediation. *Applied Catalysis B: Environmental*, 2017. 219: p. 241-248.
34. Jiang, W., X. Yin, F. Xin, Y. Bi, Y. Liu, and X. Li, Preparation of CdIn₂S₄ microspheres and application for photocatalytic reduction of carbon dioxide. *Applied Surface Science*, 2014. 288: p. 138-142.
35. Jiao, X., Z. Chen, X. Li, Y. Sun, S. Gao, W. Yan, C. Wang, Q. Zhang, Y. Lin, and Y. Luo, Defect-Mediated Electron–Hole Separation in One-Unit-Cell ZnIn₂S₄ Layers for Boosted Solar-Driven CO₂ Reduction. *Journal of the American Oil Chemists' Society*, 2017. 139(22): p. 7586-7594.
36. Tahir, M., Hierarchical 3D VO₂/ZnV₂O₄ Microspheres as an Excellent Visible Light Photocatalyst for CO₂ Reduction to Solar Fuels. *Applied Surface Science*, 2018. 468: p. 1170-1180.
37. Li, Y., X. Wu, W. Ho, K. Lv, Q. Li, M. Li, and S.C. Lee, Graphene-induced formation of visible-light-responsive SnO₂-Zn₂SnO₄ Z-scheme photocatalyst with surface vacancy for the enhanced photoreactivity towards NO and acetone oxidation. *Chemical Engineering Journal*, 2018. 336: p. 200-210.

38. Butt, F.K., C. Cao, Q. Wan, P. Li, F. Idrees, M. Tahir, W.S. Khan, Z. Ali, M.J. Zapata, and M. Safdar, Synthesis, evolution and hydrogen storage properties of ZnV_2O_4 glomerulus nano/microspheres: A prospective material for energy storage. *International Journal of Hydrogen Energy*, 2014. 39(15): p. 7842-7851.
39. Butt, F.K., C. Cao, R. Ahmed, W.S. Khan, T. Cao, N. Bidin, P. Li, Q. Wan, X. Qu, and M. Tahir, Synthesis of novel ZnV_2O_4 spinel oxide nanosheets and their hydrogen storage properties. *CrystEngComm*, 2014. 16(5): p. 894-899.
40. Duan, F., W. Dong, D. Shi, and M. Chen, Template-free synthesis of ZnV_2O_4 hollow spheres and their application for organic dye removal. *Applied Surface Science*, 2011. 258(1): p. 189-195.
41. Butt, F.K., C. Cao, Q. Wan, P. Li, F. Idrees, M. Tahir, W.S. Khan, Z. Ali, M.J. Zapata, and M. Safdar, Synthesis, evolution and hydrogen storage properties of ZnV_2O_4 glomerulus nano/microspheres: A prospective material for energy storage. *international journal of hydrogen energy*, 2014. 39(15): p. 7842-7851.
42. Wang, Z.-Y., H.-C. Chou, J.C. Wu, D.P. Tsai, and G. Mul, CO_2 photoreduction using $\text{NiO}/\text{InTaO}_4$ in optical-fiber reactor for renewable energy. *Applied Catalysis A: General*, 2010. 380(1-2): p. 172-177.
43. Nguyen, T.-V. and J.C. Wu, Photoreduction of CO_2 to fuels under sunlight using optical-fiber reactor. *Solar energy materials and solar cells*, 2008. 92(8): p. 864-872.
44. Liou, P.-Y., S.-C. Chen, J.C. Wu, D. Liu, S. Mackintosh, M. Maroto-Valer, and R. Linforth, Photocatalytic CO_2 reduction using an internally illuminated monolith photoreactor. *Energy & Environmental Science*, 2011. 4(4): p. 1487-1494.
45. Du, P., J.T. Carneiro, J.A. Moulijn, and G. Mul, A novel photocatalytic monolith reactor for multiphase heterogeneous photocatalysis. *Applied Catalysis A: General*, 2008. 334(1-2): p. 119-128.
46. Kočí, K., M. Reli, O. Kozák, Z. Lacný, D. Plachá, P. Praus, and L. Obalová, Influence of reactor geometry on the yield of CO_2 photocatalytic reduction. *Catalysis today*, 2011. 176(1): p. 212-214.
47. Anpo, M., Y. Ichihashi, M. Takeuchi, and H. Yamashita, Design of unique titanium oxide photocatalysts by an advanced metal ion-implantation method

- and photocatalytic reactions under visible light irradiation. *Research on chemical intermediates*, 1998. 24(2): p. 143-149.
48. Stroyuk, A., A. Kryukov, S.Y. Kuchmii, and V. Pokhodenko, Semiconductor photocatalytic systems for the production of hydrogen by the action of visible light. *Theoretical and Experimental Chemistry*, 2009. 45(4): p. 209.
 49. Fox, M.A. and M.T. Dulay, Heterogeneous photocatalysis. *Chemical reviews*, 1993. 93(1): p. 341-357.
 50. Kočí, K., L. Obalová, and Z. Lacný, Photocatalytic reduction of CO₂ over TiO₂ based catalysts. *Chemical Papers*, 2008. 62(1): p. 1-9.
 51. Varghese, O.K., M. Paulose, T.J. LaTempa, and C.A. Grimes, High-rate solar photocatalytic conversion of CO₂ and water vapor to hydrocarbon fuels. *Nano letters*, 2009. 9(2): p. 731-737.
 52. Zhou, D.-D., C.-T. He, P.-Q. Liao, W. Xue, W.-X. Zhang, H.-L. Zhou, J.-P. Zhang, and X.-M. Chen, A flexible porous Cu (ii) bis-imidazolate framework with ultrahigh concentration of active sites for efficient and recyclable CO₂ capture. *Chemical Communications*, 2013. 49(100): p. 11728-11730.
 53. Izumi, Y., Recent advances in the photocatalytic conversion of carbon dioxide to fuels with water and/or hydrogen using solar energy and beyond. *Coordination Chemistry Reviews*, 2013. 257(1): p. 171-186.
 54. Kumar, P., C. Joshi, A. Barras, B. Sieber, A. Addad, L. Boussekey, S. Szunerits, R. Boukherroub, and S.L. Jain, Core-shell structured reduced graphene oxide wrapped magnetically separable rGO@CuZnO@Fe₃O₄ microspheres as superior photocatalyst for CO₂ reduction under visible light. *Applied Catalysis B: Environmental*, 2017. 205: p. 654-665.
 55. Mahmodi, G., S. Sharifnia, F. Rahimpour, and S. Hosseini, Photocatalytic conversion of CO₂ and CH₄ using ZnO coated mesh: effect of operational parameters and optimization. *Solar Energy Materials and Solar Cells*, 2013. 111: p. 31-40.
 56. Winner, B., R. Jappelli, S.K. Maji, P.A. Desplats, L. Boyer, S. Aigner, C. Hetzer, T. Loher, M. Vilar, and S. Campioni, In vivo demonstration that α -synuclein oligomers are toxic. *Proceedings of the National Academy of Sciences*, 2011. 108(10): p. 4194-4199.
 57. Das, A., F. Khan, A. Sampath, and H.-J. Su. *Adaptive, asynchronous incremental redundancy (A/sup2/IR) with fixed transmission time intervals*

- (TTI) for HSDPA. in *Personal, Indoor and Mobile Radio Communications, 2002. The 13th IEEE International Symposium on*. 2002. IEEE.
58. Di Paola, A., E. García-López, G. Marcì, and L. Palmisano, A survey of photocatalytic materials for environmental remediation. *Journal of hazardous materials*, 2012. 211: p. 3-29.
 59. Moezzi, A., A.M. McDonagh, and M.B. Cortie, Zinc oxide particles: Synthesis, properties and applications. *Chemical Engineering Journal*, 2012. 185: p. 1-22.
 60. Brus, L.E., Electron–electron and electron-hole interactions in small semiconductor crystallites: The size dependence of the lowest excited electronic state. *The Journal of chemical physics*, 1984. 80(9): p. 4403-4409.
 61. Li, J. and N. Wu, Semiconductor-based photocatalysts and photoelectrochemical cells for solar fuel generation: a review. *Catalysis Science & Technology*, 2015. 5(3): p. 1360-1384.
 62. Liu, B., X. Zhao, C. Terashima, A. Fujishima, and K. Nakata, Thermodynamic and kinetic analysis of heterogeneous photocatalysis for semiconductor systems. *Physical Chemistry Chemical Physics*, 2014. 16(19): p. 8751-8760.
 63. Wu, J. and H.-M. Lin, Photo reduction of CO₂ to methanol via TiO₂ photocatalyst. *International Journal of Photoenergy*, 2005. 7(3): p. 115-119.
 64. Anpo, M., Photocatalytic reduction of CO₂ with H₂O on highly dispersed Ti-oxide catalysts as a model of artificial photosynthesis. *Journal of CO₂ Utilization*, 2013. 1: p. 8-17.
 65. Tahir, M. and N.S. Amin, Advances in visible light responsive titanium oxide-based photocatalysts for CO₂ conversion to hydrocarbon fuels. *Energy Conversion and Management*, 2013. 76: p. 194-214.
 66. Xu, F., J. Zhang, B. Zhu, J. Yu, and J. Xu, CuInS₂ sensitized TiO₂ hybrid nanofibers for improved photocatalytic CO₂ reduction. *Applied Catalysis B: Environmental*, 2018. 230: p. 194-202.
 67. Yang, G., D. Chen, H. Ding, J. Feng, J.Z. Zhang, Y. Zhu, S. Hamid, and D.W. Bahnemann, Well-designed 3D ZnIn₂S₄ nanosheets/TiO₂ nanobelts as direct Z-scheme photocatalysts for CO₂ photoreduction into renewable hydrocarbon fuel with high efficiency. *Applied Catalysis B: Environmental*, 2017. 219: p. 611-618.

68. Halmann, M., Photoelectrochemical reduction of aqueous carbon dioxide on p-type gallium phosphide in liquid junction solar cells. *Nature*, 1978. 275(5676): p. 115.
69. Inoue, T., A. Fujishima, S. Konishi, and K. Honda, Photoelectrocatalytic reduction of carbon dioxide in aqueous suspensions of semiconductor powders. *Nature*, 1979. 277(5698): p. 637.
70. Canfield, D. and K. Frese Jr, Reduction of carbon dioxide to methanol on n- and p-GaAs and p-InP. Effect of crystal face, electrolyte and current density. *Journal of the Electrochemical Society*, 1983. 130(8): p. 1772-1773.
71. Aurian-Blajeni, B., M. Halmann, and J. Manassen, Electrochemical measurement on the photoelectrochemical reduction of aqueous carbon dioxide on p-Gallium phosphide and p-Gallium arsenide semiconductor electrodes. *Solar Energy Materials*, 1983. 8(4): p. 425-440.
72. Ichikawa, S. and R. Doi, Hydrogen production from water and conversion of carbon dioxide to useful chemicals by room temperature photoelectrocatalysis. *Catalysis today*, 1996. 27(1-2): p. 271-277.
73. Fang, Z., S. Li, Y. Gong, W. Liao, S. Tian, C. Shan, and C. He, Comparison of catalytic activity of carbon-based AgBr nanocomposites for conversion of CO₂ under visible light. *Journal of Saudi Chemical Society*, 2014. 18(4): p. 299-307.
74. Dai, W., X. Hu, T. Wang, W. Xiong, X. Luo, and J. Zou, Hierarchical CeO₂/Bi₂MoO₆ heterostructured nanocomposites for photoreduction of CO₂ into hydrocarbons under visible light irradiation. *Applied Surface Science*, 2018. 434: p. 481-491.
75. Jiang, Z., X. Liang, H. Zheng, Y. Liu, Z. Wang, P. Wang, X. Zhang, X. Qin, Y. Dai, and M.-H. Whangbo, Photocatalytic reduction of CO₂ to methanol by three-dimensional hollow structures of Bi₂WO₆ quantum dots. *Applied Catalysis B: Environmental*, 2017. 219: p. 209-215.
76. Jin, J. and T. He, Facile synthesis of Bi₂S₃ nanoribbons for photocatalytic reduction of CO₂ into CH₃OH. *Applied Surface Science*, 2017. 394: p. 364-370.
77. Li, H., C. Li, L. Han, C. Li, and S. Zhang, Photocatalytic reduction of CO₂ with H₂O on CuO/TiO₂ catalysts. *Energy Sources, Part A: Recovery, Utilization, and Environmental Effects*, 2016. 38(3): p. 420-426.

78. Prasad, D.R., N.S.B. Rahmat, H.R. Ong, C.K. Cheng, M.R. Khan, and D. Sathiyamoorthy, Preparation and Characterization of Photocatalyst for the Conversion of Carbon Dioxide to Methanol. *World Academy of Science, Engineering and Technology, International Journal of Chemical, Molecular, Nuclear, Materials and Metallurgical Engineering*, 2016. 10(5): p. 552-555.
79. Xiang, T., F. Xin, J. Chen, Y. Wang, X. Yin, and X. Shao, Selective photocatalytic reduction of CO₂ to methanol in CuO-loaded NaTaO₃ nanocubes in isopropanol. *Beilstein journal of nanotechnology*, 2016. 7(1): p. 776-783.
80. Gusain, R., P. Kumar, O.P. Sharma, S.L. Jain, and O.P. Khatri, Reduced graphene oxide–CuO nanocomposites for photocatalytic conversion of CO₂ into methanol under visible light irradiation. *Applied Catalysis B: Environmental*, 2016. 181: p. 352-362.
81. Zhang, L., N. Li, H. Jiu, G. Qi, and Y. Huang, ZnO-reduced graphene oxide nanocomposites as efficient photocatalysts for photocatalytic reduction of CO₂. *Ceramics International*, 2015. 41(5): p. 6256-6262.
82. Liu, E., L. Kang, F. Wu, T. Sun, X. Hu, Y. Yang, H. Liu, and J. Fan, Photocatalytic reduction of CO₂ into methanol over Ag/TiO₂ nanocomposites enhanced by surface plasmon resonance. *Plasmonics*, 2014. 9(1): p. 61-70.
83. Baeissa, E., Green synthesis of methanol by photocatalytic reduction of CO₂ under visible light using a graphene and tourmaline co-doped titania nanocomposites. *Ceramics international*, 2014. 40(8): p. 12431-12438.
84. Kumar, P., B. Sain, and S.L. Jain, Photocatalytic reduction of carbon dioxide to methanol using a ruthenium trinuclear polyazine complex immobilized on graphene oxide under visible light irradiation. *Journal of Materials Chemistry A*, 2014. 2(29): p. 11246-11253.
85. Tang, C., W. Hou, E. Liu, X. Hu, and J. Fan, CeF₃/TiO₂ composite as a novel visible-light-driven photocatalyst based on upconversion emission and its application for photocatalytic reduction of CO₂. *Journal of Luminescence*, 2014. 154: p. 305-309.
86. Ohno, T., N. Murakami, T. Koyanagi, and Y. Yang, Photocatalytic reduction of CO₂ over a hybrid photocatalyst composed of WO₃ and graphitic carbon nitride (g-C₃N₄) under visible light. *Journal of CO₂ Utilization*, 2014. 6: p. 17-25.

87. Li, X., H. Liu, D. Luo, J. Li, Y. Huang, H. Li, Y. Fang, Y. Xu, and L. Zhu, Adsorption of CO₂ on heterostructure CdS (Bi₂S₃)/TiO₂ nanotube photocatalysts and their photocatalytic activities in the reduction of CO₂ to methanol under visible light irradiation. *Chemical Engineering Journal*, 2012. 180: p. 151-158.
88. Truong, Q.D., J.-Y. Liu, C.-C. Chung, and Y.-C. Ling, Photocatalytic reduction of CO₂ on FeTiO₃/TiO₂ photocatalyst. *Catalysis Communications*, 2012. 19: p. 85-89.
89. Krejčíková, S., L. Matějová, K. Kočí, L. Obalová, Z. Matěj, L. Čapek, and O. Šolcová, Preparation and characterization of Ag-doped crystalline titania for photocatalysis applications. *Applied Catalysis B: Environmental*, 2012. 111: p. 119-125.
90. Kočí, K., V. Matějka, P. Kovář, Z. Lacný, and L. Obalová, Comparison of the pure TiO₂ and kaolinite/TiO₂ composite as catalyst for CO₂ photocatalytic reduction. *Catalysis Today*, 2011. 161(1): p. 105-109.
91. Gondal, M.A., M.A. Ali, M.A. Dastageer, and X. Chang, CO₂ conversion into methanol using granular silicon carbide (α 6H-SiC): A comparative evaluation of 355 nm Laser and Xenon mercury broad band radiation sources. *Catalysis letters*, 2013. 143(1): p. 108-117.
92. Wang, X., K. Maeda, A. Thomas, K. Takanabe, G. Xin, J.M. Carlsson, K. Domen, and M. Antonietti, A metal-free polymeric photocatalyst for hydrogen production from water under visible light. *Nature materials*, 2009. 8(1): p. 76-80.
93. Wang, C., R.L. Thompson, J. Baltrus, and C. Matranga, Visible light photoreduction of CO₂ using CdSe/Pt/TiO₂ heterostructured catalysts. *The Journal of Physical Chemistry Letters*, 2009. 1(1): p. 48-53.
94. Liao, G., S. Chen, X. Quan, H. Yu, and H. Zhao, Graphene oxide modified gC₃N₄ hybrid with enhanced photocatalytic capability under visible light irradiation. *Journal of Materials Chemistry*, 2012. 22(6): p. 2721-2726.
95. Hou, Y., Z. Wen, S. Cui, X. Guo, and J. Chen, Constructing 2D Porous Graphitic C₃N₄ Nanosheets/Nitrogen-Doped Graphene/Layered MoS₂ Ternary Nanojunction with Enhanced Photoelectrochemical Activity. *Advanced materials*, 2013. 25(43): p. 6291-6297.

96. Chen, L., X. Zeng, P. Si, Y. Chen, Y. Chi, D.-H. Kim, and G. Chen, Gold nanoparticle-graphite-like C_3N_4 nanosheet nanohybrids used for electrochemiluminescent immunosensor. *Analytical chemistry*, 2014. 86(9): p. 4188-4195.
97. Yan, R., D. Gargas, and P. Yang, Nanowire photonics. *Nature photonics*, 2009. 3(10): p. 569-576.
98. Lin, Y., G. Yuan, R. Liu, S. Zhou, S.W. Sheehan, and D. Wang, Semiconductor nanostructure-based photoelectrochemical water splitting: a brief review. *Chemical Physics Letters*, 2011. 507(4): p. 209-215.
99. Sun, J.-X., Y.-P. Yuan, L.-G. Qiu, X. Jiang, A.-J. Xie, Y.-H. Shen, and J.-F. Zhu, Fabrication of composite photocatalyst g- C_3N_4 -ZnO and enhancement of photocatalytic activity under visible light. *Dalton Transactions*, 2012. 41(22): p. 6756-6763.
100. Xu, X., G. Liu, C. Randorn, and J.T. Irvine, g- C_3N_4 coated SrTiO₃ as an efficient photocatalyst for H₂ production in aqueous solution under visible light irradiation. *international journal of hydrogen energy*, 2011. 36(21): p. 13501-13507.
101. Yan, H. and H. Yang, TiO₂-g- C_3N_4 composite materials for photocatalytic H₂ evolution under visible light irradiation. *Journal of alloys and compounds*, 2011. 509(4): p. L26-L29.
102. Mao, J., T. Peng, X. Zhang, K. Li, L. Ye, and L. Zan, Effect of graphitic carbon nitride microstructures on the activity and selectivity of photocatalytic CO₂ reduction under visible light. *Catalysis Science & Technology*, 2013. 3(5): p. 1253-1260.
103. Wang, Y., X. Wang, and M. Antonietti, Polymeric graphitic carbon nitride as a heterogeneous organocatalyst: from photochemistry to multipurpose catalysis to sustainable chemistry. *Angewandte Chemie International Edition*, 2012. 51(1): p. 68-89.
104. Martin-Gil, J., F. Martin-Gil, E. Moran, M. Miki-Yoshida, L. Martinez, and M. José-Yacamán, Synthesis of low density and high hardness carbon spheres containing nitrogen and oxygen. *Acta metallurgica et materialia*, 1995. 43(3): p. 1243-1247.
105. Zhou, S., Y. Liu, J. Li, Y. Wang, G. Jiang, Z. Zhao, D. Wang, A. Duan, J. Liu, and Y. Wei, Facile in situ synthesis of graphitic carbon nitride (g- C_3N_4)-N-

- TiO₂ heterojunction as an efficient photocatalyst for the selective photoreduction of CO₂ to CO. *Applied Catalysis B: Environmental*, 2014. 158: p. 20-29.
106. Pei, L., N. Lin, T. Wei, H. Liu, and H. Yu, Zinc vanadate nanorods and their visible light photocatalytic activity. *Journal of Alloys and Compounds*, 2015. 631: p. 90-98.
 107. Xie, Q., F. Li, H. Guo, L. Wang, Y. Chen, G. Yue, and D.-L. Peng, Template-free synthesis of amorphous double-shelled zinc–cobalt citrate hollow microspheres and their transformation to crystalline ZnCo₂O₄ microspheres. *ACS applied materials & interfaces*, 2013. 5(12): p. 5508-5517.
 108. Xu, S. and D.D. Sun, Significant improvement of photocatalytic hydrogen generation rate over TiO₂ with deposited CuO. *International Journal of Hydrogen Energy*, 2009. 34(15): p. 6096-6104.
 109. Butt, F.K., M. Tahir, C. Cao, F. Idrees, R. Ahmed, W.S. Khan, Z. Ali, N. Mahmood, M. Tanveer, and A. Mahmood, Synthesis of novel ZnV₂O₄ hierarchical nanospheres and their applications as electrochemical supercapacitor and hydrogen storage material. *ACS applied materials & interfaces*, 2014. 6(16): p. 13635-13641.
 110. Ullah, K., S. Ye, L. Zhu, S.B. Jo, W.K. Jang, K.-Y. Cho, and W.-C. Oh, Noble metal doped graphene nanocomposites and its study of photocatalytic hydrogen evolution. *Solid State Sciences*, 2014. 31: p. 91-98.
 111. Ke, J., X. Duan, S. Luo, H. Zhang, H. Sun, J. Liu, M. Tade, and S. Wang, UV-assisted construction of 3D hierarchical rGO/Bi₂MoO₆ composites for enhanced photocatalytic water oxidation. *Chemical Engineering Journal*, 2017. 313: p. 1447-1453.
 112. Tonda, S., S. Kumar, Y. Gawli, M. Bhardwaj, and S. Ogale, g-C₃N₄ (2D)/CdS (1D)/rGO (2D) dual-interface nano-composite for excellent and stable visible light photocatalytic hydrogen generation. *International Journal of Hydrogen Energy*, 2017. 42(9): p. 5971-5984.
 113. Zhang, L., N. Li, H. Jiu, G. Qi, and Y. Huang, ZnO-reduced graphene oxide nanocomposites as efficient photocatalysts for photocatalytic reduction of CO₂. *Ceramics International*, 2015. 41(5): p. 6256-6262.
 114. Tan, L.-L., W.-J. Ong, S.-P. Chai, and A.R. Mohamed, Reduced graphene oxide-TiO₂ nanocomposite as a promising visible-light-active photocatalyst for

- the conversion of carbon dioxide. *Nanoscale research letters*, 2013. 8(1): p. 465.
115. Wang, P.-Q., Y. Bai, P.-Y. Luo, and J.-Y. Liu, Graphene–WO₃ nanobelt composite: Elevated conduction band toward photocatalytic reduction of CO₂ into hydrocarbon fuels. *Catalysis Communications*, 2013. 38: p. 82-85.
 116. Yu, J., J. Jin, B. Cheng, and M. Jaroniec, A noble metal-free reduced graphene oxide–CdS nanorod composite for the enhanced visible-light photocatalytic reduction of CO₂ to solar fuel. *Journal of Materials Chemistry A*, 2014. 2(10): p. 3407.
 117. Zhou, P., J. Yu, and M. Jaroniec, All-solid-state Z-scheme photocatalytic systems. *Advanced Materials*, 2014. 26(29): p. 4920-4935.
 118. Bao, Y. and K. Chen, Novel Z-scheme BiOBr/reduced graphene oxide/protonated g-C₃N₄ photocatalyst: Synthesis, characterization, visible light photocatalytic activity and mechanism. *Applied Surface Science*, 2018. 437: p. 51-61.
 119. Jo, W.-K., S. Kumar, S. Eslava, and S. Tonda, Construction of Bi₂WO₆/RGO/g-C₃N₄ 2D/2D/2D hybrid Z-scheme heterojunctions with large interfacial contact area for efficient charge separation and high-performance photoreduction of CO₂ and H₂O into solar fuels. *Applied Catalysis B: Environmental*, 2018. 239: p. 586-598.
 120. Wang, C., G. Wang, X. Zhang, X. Dong, C. Ma, X. Zhang, H. Ma, and M. Xue, Construction of g-C₃N₄ and FeWO₄ Z-scheme photocatalyst: effect of contact ways on the photocatalytic performance. *RSC Advances*, 2018. 8(33): p. 18419-18426.
 121. Xue, W., X. Hu, E. Liu, and J. Fan, Novel reduced graphene oxide-supported Cd_{0.5}Zn_{0.5}S/g-C₃N₄ Z-scheme heterojunction photocatalyst for enhanced hydrogen evolution. *Applied Surface Science*, 2018. 447: p. 783-794.
 122. Ma, D., J. Wu, M. Gao, Y. Xin, T. Ma, and Y. Sun, Fabrication of Z-scheme g-C₃N₄/RGO/Bi₂WO₆ photocatalyst with enhanced visible-light photocatalytic activity. *Chemical Engineering Journal*, 2016. 290: p. 136-146.
 123. Iwase, A., Y.H. Ng, Y. Ishiguro, A. Kudo, and R. Amal, Reduced graphene oxide as a solid-state electron mediator in Z-scheme photocatalytic water splitting under visible light. *Journal of the American Chemical Society*, 2011. 133(29): p. 11054-11057.

124. Low, J., C. Jiang, B. Cheng, S. Wageh, A.A. Al-Ghamdi, and J. Yu, A Review of Direct Z-Scheme Photocatalysts. *Small Methods*, 2017.
125. Yu, W., D. Xu, and T. Peng, Enhanced photocatalytic activity of g-C₃N₄ for selective CO₂ reduction to CH₃OH via facile coupling of ZnO: a direct Z-scheme mechanism. *Journal of Materials Chemistry A*, 2015. 3(39): p. 19936-19947.
126. Chen, F., Q. Yang, X. Li, G. Zeng, D. Wang, C. Niu, J. Zhao, H. An, T. Xie, and Y. Deng, Hierarchical assembly of graphene-bridged Ag₃PO₄/Ag/BiVO₄ (040) Z-scheme photocatalyst: an efficient, sustainable and heterogeneous catalyst with enhanced visible-light photoactivity towards tetracycline degradation under visible light irradiation. *Applied Catalysis B: Environmental*, 2017. 200: p. 330-342.
127. Jiang, D., W. Ma, P. Xiao, L. Shao, D. Li, and M. Chen, Enhanced photocatalytic activity of graphitic carbon nitride/carbon nanotube/Bi₂WO₆ ternary Z-scheme heterojunction with carbon nanotube as efficient electron mediator. *Journal of Colloid and Interface Science*, 2018. 512: p. 693-700.
128. de Lasa, H., B. Serrano, and M. Salaiques, *Novel photocatalytic reactors for water and air treatment*, in *Photocatalytic Reaction Engineering*. 2005, Springer. p. 17-47.
129. Ola, O. and M.M. Maroto-Valer, Review of material design and reactor engineering on TiO₂ photocatalysis for CO₂ reduction. *Journal of Photochemistry and Photobiology C: Photochemistry Reviews*, 2015. 24: p. 16-42.
130. Tahir, B., M. Tahir, and N.S. Amin, Gold–indium modified TiO₂ nanocatalysts for photocatalytic CO₂ reduction with H₂ as reductant in a monolith photoreactor. *Applied Surface Science*, 2015. 338: p. 1-14.
131. Ampelli, C., C. Genovese, R. Passalacqua, S. Perathoner, and G. Centi, The use of a solar photoelectrochemical reactor for sustainable production of energy. *Theoretical Foundations of Chemical Engineering*, 2012. 46(6): p. 651-657.
132. Tan, S.S., L. Zou, and E. Hu, Photocatalytic reduction of carbon dioxide into gaseous hydrocarbon using TiO₂ pellets. *Catalysis Today*, 2006. 115(1-4): p. 269-273.

133. Sharma, A. and B.-K. Lee, Photocatalytic reduction of carbon dioxide to methanol using nickel-loaded TiO₂ supported on activated carbon fiber. *Catalysis Today*, 2017. 298: p. 158-167.
134. Xiong, Z., Z. Lei, S. Ma, X. Chen, B. Gong, Y. Zhao, J. Zhang, C. Zheng, and J.C. Wu, Photocatalytic CO₂ reduction over V and W codoped TiO₂ catalyst in an internal-illuminated honeycomb photoreactor under simulated sunlight irradiation. *Applied Catalysis B: Environmental*, 2017. 219: p. 412-424.
135. Song, G., F. Xin, and X. Yin, Photocatalytic reduction of carbon dioxide over ZnFe₂O₄/TiO₂ nanobelts heterostructure in cyclohexanol. *Journal of colloid and interface science*, 2015. 442: p. 60-66.
136. Kočí, K., L. Obalová, D. Plachá, and Z. Lacný, Effect of temperature, pressure and volume of reacting phase on photocatalytic CO₂ reduction on suspended nanocrystalline TiO₂. *Collection of czechoslovak chemical communications*, 2008. 73(8): p. 1192-1204.
137. Koci, K., L. Obalova, and O. Solcova, Kinetic study of photocatalytic reduction of CO₂ over TiO₂. *Chemical and Process Engineering*, 2010. 31: p. 395-407.
138. Davis, M.E. and R.J. Davis, *Fundamentals of chemical reaction engineering*. 2012: Courier Corporation.
139. Tan, S.S., L. Zou, and E. Hu, Kinetic modelling for photosynthesis of hydrogen and methane through catalytic reduction of carbon dioxide with water vapour. *Catalysis Today*, 2008. 131(1-4): p. 125-129.
140. Yin, Z., J. Qin, W. Wang, and M. Cao, Rationally designed hollow precursor-derived Zn₃V₂O₈ nanocages as a high-performance anode material for lithium-ion batteries. *Nano Energy*, 2017. 31: p. 367-376.
141. Zhang, T., Y. Shen, Y. Qiu, Y. Liu, R. Xiong, J. Shi, and J. Wei, Facial synthesis and photoreaction mechanism of BiFeO₃/Bi₂Fe₄O₉ heterojunction nanofibers. *ACS Sustainable Chemistry & Engineering*, 2017. 5(6): p. 4630-4636.
142. Lv, H., X. Wu, Y. Liu, Y. Cao, and H. Ren, In situ synthesis of ternary Zn_{0.5}Cd_{0.5}S (0D)/RGO (2D)/g-C₃N₄ (2D) heterostructures with efficient photocatalytic H₂ generation activity. *Materials Letters*, 2019. 236: p. 690-693.
143. Bai, J., X. Li, G. Liu, Y. Qian, and S. Xiong, Unusual Formation of ZnCo₂O₄ 3D Hierarchical Twin Microspheres as a High-Rate and Ultralong-Life

- Lithium-Ion Battery Anode Material. *Advanced Functional Materials*, 2014. 24(20): p. 3012-3020.
144. Shahid, M., J. Liu, Z. Ali, I. Shakir, and M.F. Warsi, Structural and electrochemical properties of single crystalline MoV₂O₈ nanowires for energy storage devices. *Journal of Power Sources*, 2013. 230: p. 277-281.
 145. Lu, X., K. Xu, P. Chen, K. Jia, S. Liu, and C. Wu, Facile one step method realizing scalable production of g-C₃N₄ nanosheets and study of their photocatalytic H₂ evolution activity. *Journal of Materials Chemistry A*, 2014. 2(44): p. 18924-18928.
 146. Hou, Y., Z. Wen, S. Cui, X. Guo, and J. Chen, Constructing 2D porous graphitic C₃N₄ nanosheets/nitrogen-doped graphene/layered MoS₂ ternary nanojunction with enhanced photoelectrochemical activity. *Advanced Materials*, 2013. 25(43): p. 6291-6297.
 147. Chang, S.-m. and W.-s. Liu, Surface doping is more beneficial than bulk doping to the photocatalytic activity of vanadium-doped TiO₂. *Applied Catalysis B: Environmental*, 2011. 101(3-4): p. 333-342.
 148. Shehzad, N., M. Tahir, K. Johari, T. Murugesan, and M. Hussain, Fabrication of highly efficient and stable indirect Z-scheme assembly of AgBr/TiO₂ via graphene as a solid-state electron mediator for visible light induced enhanced photocatalytic H₂ production. *Applied Surface Science*, 2019. 463: p. 445-455.
 149. Tahir, M., B. Tahir, N.A.S. Amin, and Z.Y. Zakaria, Photo-induced reduction of CO₂ to CO with hydrogen over plasmonic Ag-NPs/TiO₂ NWs core/shell hetero-junction under UV and visible light. *Journal of CO₂ Utilization*, 2017. 18: p. 250-260.
 150. Hu, X., X. Liu, J. Tian, Y. Li, and H. Cui, Towards full-spectrum (UV, visible, and near-infrared) photocatalysis: achieving an all-solid-state Z-scheme between Ag₂O and TiO₂ using reduced graphene oxide as the electron mediator. *Catalysis Science & Technology*, 2017. 7(18): p. 4193-4205.
 151. Chong, S., S. Wang, M. Tadé, H.M. Ang, and V. Pareek, Simulations of photodegradation of toluene and formaldehyde in a monolith reactor using computational fluid dynamics. *AIChE journal*, 2011. 57(3): p. 724-734.